A general self-dual adaptative filtering toggle operator

Leyza Baldo Dorini Neucimar Jerônimo Leite
Institute of Computing, P.O.Box: 6176,
University of Campinas - UNICAMP,
13084-971, Campinas, SP, Brazil
E-mail: {ldorini, neucimar}@ic.unicamp.br

Abstract

In the mathematical morphology context, a filter is an operator that is increasing and idempotent. We propose an alternative way to build self-dual morphological filters, extending some results obtained for morphological centers to a different class of toggle operators whose decision rule is based on which primitive value is closer to the original one. With this new approach, a wider range of primitives can be considered without causing oscillations, a common problem in toggle mappings. We also explore the use of non-flat structuring elements which are shown to produce sharper filtered images. To evaluate the proposed approach, we carry out tests on images with different kinds of noise using different pairs of primitives. Experimental tests on Synthetic Aperture Radar (SAR) images show promising results, outperforming some well-known filters related to this type of pictures.

1 Introduction

A morphological filter is defined as an operator, ρ, acting on a complete lattice $\mathcal{L}$ that preserves the ordering $\leq$ of $\mathcal{L}$, $X \leq Y \Rightarrow \rho(X) \leq \rho(Y)$, and is idempotent, $\rho(\rho(X)) = \rho(X)$. The first condition, usually referred as increasingness, preserves the basic lattice features, while the second one is due to the fact that increasing operations are non reversible and loose information [10].

There are also some other desired properties such as self-duality, that is, $\rho^* = \rho$, where $\rho^*(X) = (\rho(X^*))^*$ is called the negative operator of ρ. A self-dual operator treats the foreground and background of an image identically.

Since its introduction in 1988, the morphological filtering theory has been widely discussed. Serra and Vincent [10] presented a tutorial on morphological filtering, approaching from the basic opening and closings operations to alternating sequential filters and toggle mappings.

In [4], Heijmans explored how to construct morphological filters and derived notions called filter-derivates, where the idempotence condition is only partially satisfied. However, as stated by the author, the proposed construction method in general yields filters that are not self-dual.

Subsequently [2], Heijmans showed how to build self-dual filters by iteration of a self-dual increasing operator using the morphological center as basis. He also generalized the notion of alternating sequential filters by using filter-derivates instead of the traditional opening and closing operations.

In the following, we present a toggle-based framework to build self-dual morphological filters. We extend the results obtained using morphological centers [2][10] to a different class of toggle operators, in which the decision rule chooses the primitive transformation that is closer to the original pixel value. We prove that, when using suitable primitives, the defined toggle operator converges pixelwise to one of the primitives, constituting an activity-extensive operator.

In contrast to other approaches, which require the definition of a self-dual operator to build self-dual filters [2], here we only require that the primitives be dual operations and bounded in a specific way. We also explore the use of non-flat structuring elements, which lead to better filtering results than the flat ones.

This paper is organized as follows. In the next section, we briefly discuss toggle operators, more specifically the morphological centers. The proposed approach and some of its main properties are described in Section 3. Section 4 shows some experimental results, analyzing how the primitives and structuring elements influence the transformation,and Section 5 presents some results of Synthetic Aperture Radar (SAR) image filtering. Finally, we draw some conclusions and future work perspectives in Section 6 .

2 Toggle Mapping and Filtering

The key idea of toggle transformations or mappings is to associate an image with (a) a series of possible transforma-

tions (primitives), φ_i, and (b) a decision rule which determines at each pixel $\mathbf{x}$ the best value among the candidates $\varphi_i(\mathbf{x})$ [10, 11].

A simple example of toggle mapping is the binary thresholding operation, where the decision rule involves, at a point $\mathbf{x}$, the value $f(\mathbf{x})$ and the threshold level. In this case, the primitives are the white and black, which are independent of $f(\mathbf{x})$. On the other hand, in some cases, the primitives consist on transformations acting on the initial image, as in morphological centers. The algorithm definition of a center, γ, for a family of primitives φ_i derives from [10]:

$$\dot{\wedge}\varphi_i = \gamma = (\mathtt{id} \vee \eta) \wedge \zeta = (\mathtt{id} \wedge \zeta) \vee \eta, \qquad (1)$$

with $\eta = \vee\varphi_i$ and $\zeta = \wedge\varphi_i$, where $\vee$ stands for $\sup$ and $\wedge$ for $\inf$.

When using only two primitives, φ_1, φ_2, the morphological center consists on the median between f, φ_1 and φ_2 [10]. The median is a self-dual nonlinear image transformation frequently used for noise filtering due to its edge preservation properties. However, it is not idempotent, and repeated applications can make previous changes undone and lead to oscillations [3].

Heijmans [2] used the morphological center to build self-dual operators and subsequently self-dual filters. Basically, he explores the fact that every increasing, self-dual operator can be modified in such a way that the sequence of iterations of a given image is pixelwise monotone (strictly increasing or decreasing in each pixel). This implies on a convergence to a limit operator that is idempotent, thus avoiding oscillation problems.

Based on these same convergence assumptions, we propose an alternative way to build self-dual morphological filters using a different class of toggle operator as basis. At this way, a wider range of primitives can be considered.

3 Proposed filtering toggle

In order to ensure a reasonable filter behavior, the primitives must have some specific properties, defined below. Here, we restrict to the use of the lattice of gray-scale images, where several definitions can be used in a more appropriate way (like negation, operators are restricted to finite window ones, and so on).

Definition 3.1. *(Bound-max transform) A transformation ψ is said* bound-max *if it is increasing and bounded below by the minimum over the neighborhood defined by the structuring element, that is*

$$[\psi(f)](\mathbf{x}) \geq \min\{\tilde{\mathbf{x}}\}\ \forall\ \tilde{\mathbf{x}} \in \mathcal{N}(\mathbf{x}), \qquad (2)$$

where $\mathcal{N}$ represents the neighborhood defined by the structuring element.

Definition 3.2. *(Bound-min transform) A transformation ϕ is said* bound-min *if it is increasing and bounded above by the maximum over the neighborhood defined by the structuring element, that is*

$$[\phi(f)](\mathbf{x}) \leq \max\{\tilde{\mathbf{x}}\}\ \forall\ \tilde{\mathbf{x}} \in \mathcal{N}(\mathbf{x}), \qquad (3)$$

where, again, $\mathcal{N}$ represents the neighborhood defined by the structuring element.

Note that these definitions are similar to that of extensive/anti-extensive transformations. We now define a toggle operator with filtering properties.

Definition 3.3. *(Toggle-filter) We call* toggle-filter *a toggle operator defined as follows*

$f^{k+1}(\mathbf{x}) =$

$$\begin{cases} [\psi(f^k)](\mathbf{x}) & \text{if } [\psi(f^k)](\mathbf{x}) - f^k(\mathbf{x}) < f^k(\mathbf{x}) - [\phi(f^k)](\mathbf{x}), \\ f^k(\mathbf{x}) & \text{if } [\psi(f^k)](\mathbf{x}) - f^k(\mathbf{x}) = f^k(\mathbf{x}) - [\phi(f^k)](\mathbf{x}), \\ [\phi(f^k)](\mathbf{x}) & \text{otherwise,} \end{cases} \qquad (4)$$

where the primitives ϕ and ψ are bound-min and bound-max, respectively. Finally, f^k is the resulting image after k iterations.

The decision rule chooses, at each point $\mathbf{x}$, the primitive transformed value that is closer to the original one, with the primitives being themselves transformations acting on the initial signal. The increasingness property preserves the partial ordering. Since not necessarily $\psi \geq \mathtt{id} \geq \phi$, we only consider values on $\mathbb{R}^+$. Also note that the toggle-filter operator it is continuous by definition.

3.1 Toggle-filter properties

In order to prove that this operator constitutes a filter, we must show that it is increasing and idempotent. In this paper, we ensure the increasingness property by considering as primitives only compositions of increasing transformations.

We have verified through computational experiments that, although the toggle-filter operator is not necessarily idempotent, it has a well-controlled behavior, with a given pixel value converging to exclusively one of the primitives after a few iterations. However, if we impose two more conditions on the primitives, we can ensure that a given pixel converges to only one primitive from the first iteration, as stated in Proposition 3.4.

Proposition 3.4. *Suppose $f^{k+1}(\mathbf{x}) = [\psi(f^k)](\mathbf{x})$. If*

1. $[\psi(f^{k+1})]([\psi(f^k)](\mathbf{x})) < 2[\psi(f^k)](\mathbf{x}) - f^k(\mathbf{x})$
2. $[\phi(f^{k+1})]([\psi(f^k)](\mathbf{x})) \leq f^k(\mathbf{x})$

then the toggle-filter operator converges pixelwise to exclusively one of the primitives through the different iterations.
PROOF. *The toggle operator defined in Eq. 4 can be easily rewritten as*

$$f^{k+1}(\mathbf{x}) = \begin{cases} [\psi(f^k)](\mathbf{x}) & \text{if } [\psi(f^k)](\mathbf{x}) + [\phi(f^k)](\mathbf{x}) < 2f^k(\mathbf{x}), \\ f^k(\mathbf{x}) & \text{if } [\psi(f^k)](\mathbf{x}) + [\phi(f^k)](\mathbf{x}) = 2f^k(\mathbf{x}), \\ [\phi(f^k)](\mathbf{x}) & \text{otherwise,} \end{cases} \quad (5)$$

We are assuming $f^{k+1}(\mathbf{x}) = [\psi(f^k)](\mathbf{x})$. So, in order to prove that the toggle operator will converge for the same primitive in the next iteration, we must show that $f^{k+2}(\mathbf{x}) = [\psi(f^{k+1})](\mathbf{x})$, that is,

$$[\psi(f^{k+1})]([\psi(f^k)](\mathbf{x})) + [\phi(f^{k+1})]([\psi(f^k)](\mathbf{x})) \leq 2[\psi(f^k)](\mathbf{x}),$$

which holds when considering conditions (1) and (2). The proof when $f^{k+1}(\mathbf{x}) = [\phi(f^k)](\mathbf{x})$ is analogous.

The condition (1) of the enunciation of Proposition 3.4 implies that the difference between successive transformed values decreases through iterations. This constitutes a pixelwise monotone (increasing or decreasing) sequence that converges to a constant value through these iterations.

Proposition 3.5. *Let ψ be bound-max. If $[\psi(f^{k+1})]([\psi(f^k)](\mathbf{x})) - [\psi(f^k)](\mathbf{x}) \leq [\psi(f^k)](\mathbf{x}) - f^k(\mathbf{x})$ (condition (1)), $(\psi)_{k=1}^{\infty}$ is monotone increasing. Thus, the sequence must converge.*
PROOF. *Take an $\epsilon > 0$ and let $c = \sup(\psi_k)$. Then c is finite, and given $\epsilon > 0$, there exists at least one integer N such that $\psi_N > c - \epsilon$. Since the sequence is monotone increasing, we then have that*

$$|c - \psi_k| < \epsilon \quad \forall\, k > N$$

what means, by definition, that the sequence converges to c. The proof corresponding to the primitive ϕ is analogous.

□

A toggle-filter operator whose primitives obey the conditions of Proposition 3.4 is said pointwise monotone, since it is either increasing or decreasing in each pixel. According to the following proposition, this also implies that it is *activity-extensive*.

Proposition 3.6. *The operator ρ is activity-extensive if and only if the sequence $\rho^n(F)$ is pointwise monotone, for every function F.*
PROOF. *See [2], Proposition 21.*

□

The activity-extensive property for the toggle-filter is more general than that of the morphological centers. When using extensive and anti-extensive primitives, for example, the image will not be filtered through morphological centers (in this case, the original image will be the invariance domain since, for two primitives, the center is nothing but the median transformation).

The following proposition gives us the necessary conditions to a filter.

Proposition 3.7. *If ρ is a continuous operator and $\rho^n \rightarrow \rho^\infty$, then ρ^∞ is idempotent. In particular, if ρ is also increasing, then ρ^∞ is a filter.*
PROOF. *See [2], Proposition 15.*

□

Now, we have the necessary results to prove that a toggle-filter is a morphological filter.

Proposition 3.8. *Let $\mathcal{T}(\mathbf{x})$ be a toggle-filter operator. If the primitives being used obey the conditions of Proposition 3.4, then $\mathcal{T}(\mathbf{x})$ is a morphological filter.*
PROOF. *First, we recall that the primitives are stationary, that is, they approach a constant value after a certain number of iterations. From our hypothesis, we are assuming that the toggle-filter operator converges pixelwise to one of the primitives. Thus, we have that the operator converges pointwise to a limit, which implies that the operator is a filter, according to Proposition 3.7.*

□

As we mentioned before, one of the desired properties of a filter is self-duality. Proposition 3.9 states that a toggle operator of the format of the toggle-filter is a self-dual operator if we use dual primitives, thus extending the results obtained for morphological centers in [2].

Proposition 3.9. *Consider two dual primitives ψ and ϕ, that is, $[\psi(f)](\mathbf{x}) = [\phi(f)]^*(\mathbf{x}^*)$. If ψ is bound-max and ϕ is bound-min, the toggle operator given by*

$$\mathcal{T}(\mathbf{x}) = \begin{cases} [\psi(f)](\mathbf{x}) & \text{if } [\psi(f)](\mathbf{x}) - f(\mathbf{x}) < f(\mathbf{x}) - [\phi(f)](\mathbf{x}), \\ f(\mathbf{x}) & \text{if } [\psi(f)](\mathbf{x}) - f(\mathbf{x}) = f(\mathbf{x}) - [\phi(f)](\mathbf{x}), \\ [\phi(f)](\mathbf{x}) & \text{otherwise,} \end{cases} \quad (6)$$

is a self-dual operator.
PROOF. *It follows directly from the complement operator definition.*

□

Filter-derivates are concepts related to filters where the idempotence condition is only partially satisfied [2][4]. In a general way, we can use as primitives different filter-derivates, in such a way that the toggle mapping chooses the one that best adapts to a given pixel. Formally:

Definition 3.10. *[4] (Def. 3.1) An increasing operator ρ on a complete lattice $\mathcal{L}$ is called*

1. *an overfilter if $\rho^2 \geq \rho$;*
2. *an underfilter if $\rho^2 \leq \rho$;*
3. *an inf-overfilter if $\rho(id \wedge \rho) = \rho$;*
4. *an sup-underfilter if $\rho(id \vee \rho) = \rho$;*
5. *an inf-filter if ρ is a filter and an inf-overfilter;*
6. *an sup-filter if ρ is a filter and a sup-underfilter;*
7. *a strong filter if ρ is both a sup-filter and inf-filter.*

From the Duality Principle [4], it follows that these definitions occur in pairs. In the next section, we present some experimental results and discuss how different parameters (primitives, structuring elements) influence the toggle-filter transformation.

4 Results

We have carried out tests on images with different types of noise, namely Gaussian (mean: 5 and variance: 2), speckle (variance: 0.04), and salt and pepper (density of noise: 0.1), illustrated in Figure 1. We apply the toggle-filter operator using different primitives and structuring elements, thus investigating their influence for each noise.

(a) original

(b) salt and pepper (RMSE 44.98)

(c) speckle (RMSE 22.08)

(d) Gaussian (RMSE 24.84)

Figure 1. Original and noisy images.

Table 1 shows the set of considered primitives, where ε: erosion, δ: dilation, α: opening, β: closing, and

$$\xi(f(\mathbf{x})) = \begin{cases} f(\mathbf{x}) & \text{if } \bar{f(\mathbf{x})}_{n\times n} < f(\mathbf{x}), \\ \bar{f(\mathbf{x})}_{n\times n} & \text{otherwise,} \end{cases} \tag{7}$$

that is, ξ is a transformation that computes the mean value of each pixel (considering a $n \times n$ window), and then replaces the values that are lower than the original ones. The primitive $\tilde{\xi}$ is analogous, but replaces the values that are greater than the original ones.

ϕ		ψ	
Primitive	Property	Primitive	Property
ε	sup-underfilter	δ	inf-overfilter
α	filter	β	filter
$\alpha\beta$	sup-filter	$\beta\alpha$	inf-filter
$\alpha\beta\alpha$	sup-filter	$\beta\alpha\beta$	inf-filter
$\varepsilon\beta$	sup-underfilter	$\delta\alpha$	inf-overfilter
$\alpha\xi$	inf-overfilter	$\xi\alpha$	overfilter
$\xi\alpha$	inf-overfilter	$\tilde{\xi}\beta$	underfilter

Table 1. Primitives considered in the tests.

The first four primitives of Table 1 obey the conditions of Proposition 3.4. Thus, for any of these pairs of primitives, the toggle-filter operator constitutes a morphological filter. For the other three primitives, the convergence to a specific primitive happens after a finite number of iterations, as we have verified through computational experiments.

Note that we have explored the combination of morphological operations with a linear function (the mean operator). It this way, we can take advantage of the well-known benefits of such a transformation on image filtering, as we will illustrate in Section 4.

Tables 2, 3 and 4 show the RMSE between the original and filtered images, using the primitives of Table 1. Observe that we obtain lower RMSE scores when using non-flat structuring elements. In the following tables, *NF line* denotes the non-flat structuring element $g_\sigma = \left[-\frac{1}{\sigma} \;\; 0 \;\; -\frac{1}{\sigma}\right]$, where σ is the scale being used. *NF* 3×3 denotes the parabolic structuring function, defined as $g_\sigma = -|\sigma|\|\mathbf{x}/\sigma\|^2$. *Flat* denotes a 3×3 flat structuring element.

Note that, in a general way, the *NF Line* structuring element conduces to better filtering results when compared to the paraboloid, mainly on images corrupted by speckle and Gaussian noise.

In summary, the non-flat structuring elements transform the image in a more efficient way, in the sense that the flat structuring element tends to preserve most of the flat zones (weaker filtering property). This can be partially explained by the sharpening properties of the non-flat structuring elements. Shavemaker et. al [9], for example, proved that toggle operators using the same decision rule as ours have sharpening properties when we consider concave structuring functions as structuring elements.

Primitives	1st iteration			3rd iteration			5th iteration		
	NF line	NF 3×3	Flat	NF line	NF 3×3	Flat	NF line	NF 3×3	Flat
ε and δ	45.839196	52.234350	54.027818	46.013350	61.283703	67.518490	46.019172	64.877638	74.934927
α and β	44.993757	45.197617	45.218715	44.993757	45.197617	45.218715	44.993757	45.197617	45.218715
$\alpha\beta$ and $\beta\alpha$	21.699680	12.951973	13.637553	19.595721	10.279760	11.565018	17.975740	9.959203	11.543946
$\alpha\beta\alpha$ and $\beta\alpha\beta$	21.699680	12.956552	13.636086	19.595721	10.286949	11.566435	17.975740	9.970478	11.545185
$\varepsilon\beta$ and $\delta\alpha$	17.704394	14.793701	15.827039	15.140607	14.000633	15.709358	15.146515	14.020200	15.844139
$\alpha\xi$ and $\xi\alpha$	14.973064	17.976085	18.013872	14.576912	14.802629	15.007235	16.323533	15.139084	15.333759
$\xi\alpha$ and $\tilde{\xi}\beta$	12.571361	16.782212	16.757288	10.782583	11.210586	11.163574	12.227002	12.652450	12.460376

Table 2. RMSE for the image with salt and pepper noise processed by the toggle-filter operator. Original RMSE: 44.98

Primitives	1st iteration			3rd iteration			5th iteration		
	NF line	NF 3×3	Flat	NF line	NF 3×3	Flat	NF line	NF 3×3	Flat
ε and δ	24.523561	30.261435	34.714058	24.809651	35.635693	46.463310	24.809942	38.150455	54.218886
α and β	22.191971	24.698720	25.086553	22.191971	24.698720	25.086553	22.191971	24.698720	25.086553
$\alpha\beta$ and $\beta\alpha$	18.899435	21.561307	22.375694	18.127552	20.704314	22.070463	18.120551	20.631190	22.052810
$\alpha\beta\alpha$ and $\beta\alpha\beta$	18.899435	21.582136	22.413713	18.127552	20.736208	22.117517	18.120551	20.667508	22.099949
$\varepsilon\beta$ and $\delta\alpha$	19.257814	21.058530	20.221082	18.090144	18.203970	17.273691	18.077752	17.670817	17.186589
$\alpha\xi$ and $\xi\alpha$	15.041276	20.545192	21.373054	14.740220	20.328898	21.663466	16.090226	20.290186	21.610729
$\xi\alpha$ and $\tilde{\xi}\beta$	15.084320	21.226537	21.629886	13.785411	19.055371	19.901742	14.567143	18.225591	19.356990

Table 3. RMSE for the image with speckle noise processed by the toggle-filter operator. Original RMSE: 22.08

Primitives	1st iteration			3rd iteration			5th iteration		
	NF line	NF 3×3	Flat	NF line	NF 3×3	Flat	NF line	NF 3×3	Flat
ε and δ	27.173707	34.656156	39.394072	27.454539	42.561361	55.180710	27.454985	46.079805	65.533397
α and β	24.935625	27.343457	27.637299	24.935625	27.343457	27.637299	24.935625	27.343457	27.637299
$\alpha\beta$ and $\beta\alpha$	19.421262	21.406255	22.062486	18.258721	19.989974	21.447274	18.213702	19.862577	21.416747
$\alpha\beta\alpha$ and $\beta\alpha\beta$	19.421262	21.445994	22.117161	18.258721	20.039343	21.518956	18.213702	19.914279	21.487230
$\varepsilon\beta$ and $\delta\alpha$	19.521073	20.930390	20.081623	18.064284	17.864865	17.195927	18.046972	17.384279	17.185158
$\alpha\xi$ and $\xi\alpha$	15.138657	20.255623	20.884832	14.859607	19.020344	20.179912	16.379387	18.812792	19.990120
$\xi\alpha$ and $\tilde{\xi}\beta$	15.353559	21.863161	22.061116	13.700294	18.611906	19.262163	14.576275	17.241844	18.417931

Table 4. RMSE for the image with Gaussian noise processed by the toggle-filter operator. Original RMSE: 24.84

Figure 2 shows the best results obtained for each type of noise illustrated in Figure 1. For the salt and pepper noise, the best result was obtained at the 5th iteration for the parabolic structuring element at scale $\sigma = 0.2$, using as primitives $\alpha\beta$ and $\beta\alpha$. For the speckle and Gaussian noises, the best results were obtained by using the non-flat line structuring element, with the primitives $\xi\alpha$ and $\tilde{\xi}\beta$, at the 3rd iteration.

We have also compared our results against the ones obtained by using the combined toggle approach [10]. Let ζ and η be two strong filters, and let (α, β) be a pair made of an opening and a closing such that $\alpha \leq \eta \leq \zeta \leq \beta$.

As an efficient definition rule, we may proceed as follows [10]:

1. When $(\eta f)(\mathbf{x}) \leq f(\mathbf{x}) \leq (\zeta f)(\mathbf{x})$, apply a contrast κ, of primitives η and ζ.

2. When $(\alpha f)(\mathbf{x}) \leq f(\mathbf{x}) < (\eta f)(\mathbf{x})$, go down to $(\alpha f)(\mathbf{x})$, except if $(\zeta f - \eta f)(\mathbf{x})$ is smaller than a fixed value d. In the latter case, go up to $(\eta f)(\mathbf{x})$.

3. When $(\zeta f)(\mathbf{x}) < f(\mathbf{x}) \leq (\beta f)(\mathbf{x})$, apply a rule similar to rule 2, possibly with a scalar d' different from d.

Table 5 presents some results for different values of d (15, 45 and 75, respectively), using a flat and the paraboloid structuring element. Also, $\zeta = \alpha\beta\alpha$ and $\eta = \beta\alpha\beta$.

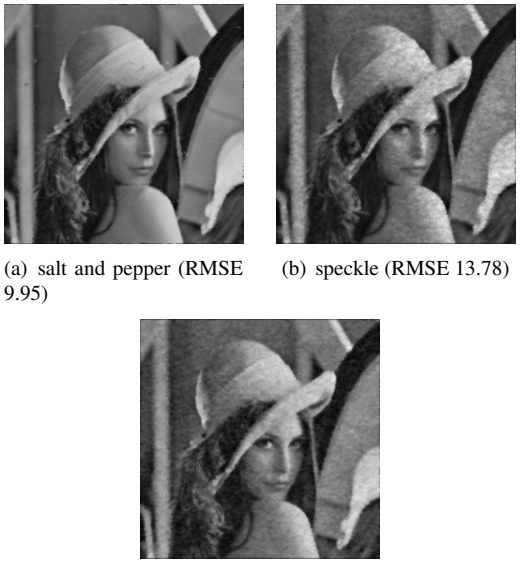

(a) salt and pepper (RMSE 9.95) (b) speckle (RMSE 13.78)

(c) Gaussian (RMSE 13.70)

Figure 2. Results with the lower RMSE.

Again, the best results were obtained when using the non-flat structuring elements. However, as one can observes in Tables 2, 3 and 4, the results obtained with our approach

Gaussian		speckle		salt and pepper	
Non-flat	Flat	Non-flat	Flat	Non-flat	Flat
25.91	27.17	23.68	24.81	24.56	29.21
20.26	24.15	21.82	23.98	15.57	20.23
19.18	22.16	20.21	22.73	12.52	16.83

Table 5. RMSE for the noisy images using the combined toggle approach.

are better for all images. For the Gaussian noise, for example, the lowest RMSE for the combined toggle approach was 19.18, against 13.70 for our approach.

In the next section, we show a "real" application of the proposed operator that helps to comprove the presented results.

5 Application: filtering of SAR images

In the last few years, the amount of images of the Earth produced by Synthetic Aperture Radar (SAR) systems has increased, as well as its applications, such as targeting, navigation and environmental monitoring. SAR can be defined as a remote sensing technology that combines reflected signals to form complex high-resolution images of broad areas of terrain. In the resulting images, a common phenomena is the presence of speckle noise, an interference pattern which effect is a granular aspect in the image. It is caused mainly by interference between coherent waves which, backscattered by natural surfaces, arrives out of phase at a point to the sensor [8].

Thus, when working with SAR images, it is essential to reduce the speckle noise in order to improve their visual quality. Besides speckle reduction, it is required that edges and details be preserved (without blurring), considering that these images are frequently used for segmentation and classification purposes [7] [8].

Various algorithms have been proposed for speckle noise reduction. Here, we compare our approach against two well-known methods: the Lee filter [5][6] and the Frost filter [1]. In SAR images it is assumed that the speckle noise has a multiplicative error model. The Lee filter first approximates this model by a linear one, and then apply the minimum square error criterion to it.

The Frost filter differs from the Lee filter in the sense that the scene reflectivity is estimated by convolving the observed image with the impulse response of the SAR system, which is obtained by minimizing the mean square error between the observed image and the scene reflectivity model. It is considered an adaptive filtering algorithm, since it adapts to the local statistics of the image to preserve edges and small features [8].

In order to compare the results obtained with our approach against the ones obtained with the Lee and Frost filters, we have used different measures, evaluating different aspects, such as the reduction of the noise and radiometric distortion [7][8]. In the following, let f be the original image, n the noisy version and $\hat{f}$ the filtered version.

The contrast ratio is a consistent measure of the effect of speckle on an image, and is given by [7]

$$\lambda = \frac{\sigma_{\hat{f}}}{\mu_{\hat{f}}} \tag{8}$$

where $\sigma_{\hat{f}}$ denotes the standard deviation and $\mu_{\hat{f}}$ the mean of $\hat{f}$. The reduction of this ratio indicates that the speckle noise has decreased.

Another measure is the mean of the ratio between the noisy and filtered pixel values. When the observed mean value differs significantly from 1 it is an indication of radiometric distortion. It is represented by the expression [7]:

$$MR = \frac{1}{NP}\sum_{k=1}^{k} r_k \tag{9}$$

where NP is the number of pixels in the image and

$$r_k = \frac{n}{\hat{f}} \tag{10}$$

We have also calculated the equivalent number of looks (ENL), given by [8]:

$$ENL = \left(\frac{\mu_{\hat{f}}}{\sigma_{\hat{f}}}\right)^2 \tag{11}$$

where, again, $\sigma_{\hat{f}}$ denotes the standard deviation and $\mu_{\hat{f}}$ the mean of $\hat{f}$. This measure indicates the number of independent intensity values averaged per pixel. Finally, we have also measured the RMSE between the original and filtered images.

We have carried out tests on three images. We have generated two test images by adding multiplicative noise to the original image f, according to the equation $n = f + ns * f$, where ns is an uniformly distributed random noise with mean 0 and variances 0.04 (Figure 3(b)) and 0.2 (Figure 3(c)). The other test image is a real SAR image (Figure 3(d)).

Table 6 presents the scores for the test images of Figure 3. We use the pair of primitives $\xi\alpha$ and $\tilde{\xi}\beta$ (which yielded the best results for the speckle noise in the experiments of Section 4), and the paraboloid structuring element at scale 30.

When compared to Lee and Frost filters, our approach presents a superior performance. When considering the λ score, for example, our approach obtained the greater reduction in all cases, indicating a speckle reduction. In a future approach, one can use as primitives statistical transformations that take into account the multiplicative model of the corresponding noise as well.

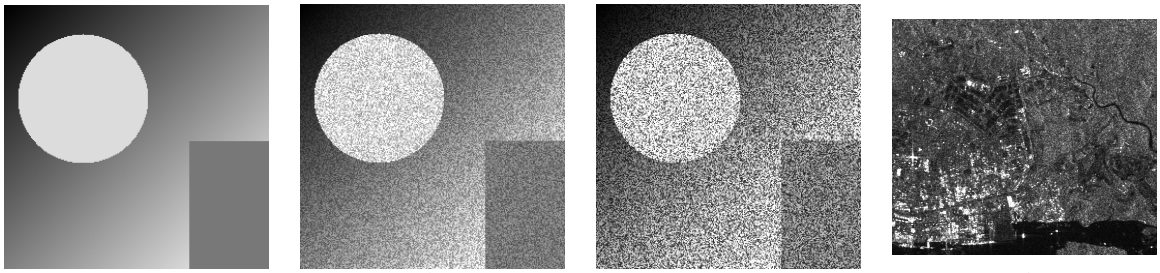

(a) (b) (c) (d)

Figure 3. Test images.

Primitives	Image1				Image2				Image3			
	Operator	Lee	Frost	Original	Operator	Lee	Frost	Original	Operator	Lee	Frost	Original
λ	0.3453	0.3669	0.3989	0.5468	0.3676	0.3737	0.3775	0.4185	0.4659	0.4991	0.5148	0.5924
ENL	8.3890	7.4293	6.2852	3.3442	7.4005	7.1616	7.0163	5.7109	4.6079	4.0143	3.7729	2.8493
MR	1.0541	1.2918	1.0766	0.9876	1.0069	1.2458	1.0026	0.9900	0.9716	1.4515	0.9615	0.9797
RMSE	21.2081	25.2486	32.1366	59.1646	12.6581	15.1425	15.5593	28.1981	-	-	-	-

Table 6. Scores for images with speckle noise processes by the toggle-filter operator.

6 Conclusions

We have proposed an alternative way to build self-dual morphological filters based on a toggle operator whose decision rule is based on which primitive value is closer to the original one. We impose some conditions on the primitives, in order to ensure an activity-extensive operator. When compared with the morphological center, another class of toggle operators used to create self-dual filters, our approach can use a wider range of primitives.

To evaluate the performance of our approach we applied the defined operator on images with different types of noise using different pairs of primitives. Promising results were obtained for all test images. As we have already discussed, the use of non-flat structuring images yields best results.

We have also shown an application of the defined operator to filter SAR images. Based on criteria that take into account different aspects, such as the reduction of the noise and radiometric distortion, our approach performed better when compared to well-known methods such as the Lee and Frost filters. This technique can be used in different applications, if we consider that the speckle noise also has a negative impact on ultrasound imaging, for example.

As a future work we intend to explore the multiscale capabilities of the non-flat structuring elements, as well as the use of different classes of primitives in a multiresolution image transformation.

Acknowledgments

The authors are grateful to FAPESP (07/52015-0; 05/04462-2) and MCT/CNPq (472402/2007-2) for the financial support of this work.

References

[1] V. Frost, J. A. Stiles, K. S. Shanmugan, and J. C. Holtzman. A model for radar image and its application to adaptive digital filtering of multiplicative noise. *IEEE Transactions on Pattern Analysis and Machine Intelligence*, 4:157–166, 1982.

[2] H. Heijmans. Morphological filters. In *Summer School on Morphological Image and Signal Processing*, 1995.

[3] H. Heijmans. Self-dual morphological operators and filters. *J. Math. Imaging Vision*, 6:15–36, 1996.

[4] H. Heijmans. Composing morphological filters. *IEEE Transactions on Image Processing*, 6:713–723, 1997.

[5] J. Lee. Digital image enhancement and noise filtering by use of local statistics. *IEEE Transactions on Pattern Analysis and Machine Intelligence*, 2:165–168, 1980.

[6] J. Lee. A simple speckle smoothing algorithm for synthetic aperture radar images. *IEEE Transactions on System, Man and Cybernetics*, 13:85–89, 1983.

[7] D. McDonald. Speckle reduction in synthetic aperture radar images. Technical Report SRL-0010-TM, Departament of Defense - Surveillance Research Laboratory, 1988.

[8] C. Oliver and S. Quegan. *Understanding Synthetic Aperture Radar Images*. SciTech Publishing, 2004.

[9] J. G. M. Schavemaker, M. J. T. Reinders, J. Gerbrands, and E. Backer. Image sharpening by morphological filtering. *Pattern Recognition*, 33:997–1012, 1999.

[10] J. Serra and L. Vincent. An overview of morphological filtering. *Circuits, Systems, and Signal Processing*, 11:47–108, 1992.

[11] P. Soille. *Morphological Image Analysis: Principles and Applications*. Springer-Verlag, 2003.